# A model for tailored-waveform radiofrequency sheaths

P. Chabert*

*LPP, CNRS, Ecole polytechnique, UPMC Univ Paris 06,*

*Univ. Paris-Sud, Observatoire de Paris, Universit Paris-Saclay,*

*Sorbonne Universites, PSL Research University,*

*Ecole polytechnique, 91128 Palaiseau, France*

M. M. Turner

*School of Physical Sciences and National Centre for Plasma Science and Technology,*

*Dublin City University, Dublin 9, Ireland*

## Abstract

The sheath physics of radiofrequency plasmas excited by a sinusoidal waveform is reasonably well understood, but existing models are complicated and not easily extended to the more complex waveforms recently introduced in applications. Turner and Chabert (Appl. Phys. Lett., **104** (2014) 164102) have proposed a model for collisionless sheaths that can easily be solved for arbitrary waveforms. In this paper we extend this model to the case of collisional sheaths in the intermediate pressure regime. Analytical expressions are derived for the electric field, the electric potential and the density profiles in the sheath region. The collisionless and collisional models are compared for a pulsed-voltage waveform.

---------

* pascal.chabert@lpp.polytechnique.fr

1

## I.   INTRODUCTION

Radiofrequency plasmas are widely used in the microelectronic industry [1, 2], and in many other applications ranging from space propulsion (see for instance [3]) to medical applications [4? –6]. In many instances, the most important phenomena take place in the radiofrequency sheaths, and it is therefore essential to appropriately model this boundary region. Historically, capacitive radiofrequency discharges were driven with a single-frequency sinusoidal waveform (typically at 13.56 MHz) and an accurate sheath model was derived for this case by Godyak [7] and Lieberman [8].

In the last two decades, it has become clear that more complex waveforms are needed to meet industrial needs. Dual-frequency excitation with two well-separated sinusoidal frequencies was first used. Robiche et al. [9] extended the Lieberman model for this case, with the approximation of small amplitude of the high-frequency component. However, more complex asymmetric waveforms were later introduced [10, 11] and the Lieberman sheath model could not be easily extended to these situations.

Two sheath models were introduced in recent years by Czarnetzki [12], and Turner and Chabert [13] to treat the more general case of arbitrary waveforms. The latter was used by Lafleur *et al.* [14] to treat the more general case of two sheaths with self-bias formation. In this paper we revisit the Turner and Chabert model and extend it to collisional sheaths. We also give more details on the derivation and on the information that can be extracted from this model. Here we do not discuss the validity of the key approximation that allows simple analytical expressions to be obtained, as this was extensively discussed in ref [13].

## II.   THE RADIOFREQUENCY SHEATH MODEL

We consider a plasma with density at the sheath edge $n_e = n_i = n_0$, electron temperature $T_e$, and a single species of positive ions with mass $M$. We assume that the plasma fills the half-plane where $x < 0$ such that the sheath starts at $x = 0$, where a flux of ions given by

$$\Gamma_i = n_0 u_B \tag{1}$$

flows into the positive half-plane $x > 0$ (here $u_B \equiv (eT_e/M)^{1/2}$ is the Bohm speed with $e$ the elementary charge and $T_e$ expressed in Volts). It follows that the sheath forms in the positive half-plane, and this sheath region will end at an electrode. The position of this

electrode, denoted by $s_m$, depends on the plasma parameters and on the voltage applied across the sheath.

We now assume that some time varying current density, $J(t)$, flows through the plasma and the sheath, and we assume that the frequency spectrum of this current permits the assumption that ions passing through the sheath respond only to the time averaged fields. Electrons, however, flow in and out of the sheath region as the current changes. In this case, we can identify a point $s(t)$, such that at any given time there is a region of positive space charge where $s(t) \leq x < s_m$ and a region of quasi-neutral plasma where $0 \leq x < s(t)$. The point denoted as $s(t)$ is understood to be the instantaneous sheath edge (this representation of the sheath is reasonable when $s_m \gg \lambda_D$). The time-averaged potential follows Poisson's equation

$$\frac{d^2\bar{\phi}}{dx^2} = -\frac{\bar{\rho}}{\epsilon_0}, \tag{2}$$

where $\epsilon_0$ is the vacuum permittivity, and the time-averaged space charge is

$$\bar{\rho} = e(n_i - \bar{n}_e). \tag{3}$$

The electronic contribution to $\bar{\rho}$ is frequently important, and generally the time-averaged electron density $\bar{n}_e$ will be the result of elaborate computations that present a major theoretical challenge. A practical approach is to make an approximation that includes the proper negative space charge within the sheath, without attempting an accurate representation of the spatial distribution of this charge. This aim is achieved by expressing the electron space charge as a constant fraction of the ion space charge,

$$\bar{n}_e = (1 - \xi)n_i, \tag{4}$$

where the dimensionless parameter $\xi$ will be computed self-consistently from the control parameters. We then have

$$\bar{\rho} = e\left[n_i - (1 - \xi)n_i\right] \tag{5}$$

$$= \xi e n_i. \tag{6}$$

This approximation leads to mutually consistent solutions for both the time-averaged and time-dependent sheath fields, without introducing any assumption about the time dependence of the sheath current or voltage, as demonstrated in Turner and Chabert [13]. Consequently, we can couple this model to an arbitrary current or voltage waveform, and proceed to construct a related sheath model, without introducing any further approximations.

In figure 1, time-averaged densities and potential in the sheaths are shown for $\xi = 0.5$ in the collisionless case, after Eqs. (11) and (12) that will be derived below. In this figure the vertical line at $s(t)/s_m$ represents the instantaneous sheath position. We will now construct the solutions for both collisionless and collisional sheaths.

## A. Collisionless sheaths

### 1. The fields

If the ions enter the sheath with a negligible velocity and are supposed to be collisionless, then energy conservation gives

$$\frac{2e\bar{\phi}}{M} + u_i^2 \approx 0, \tag{7}$$

and flux conservation implies

$$u_i n_i = u_B n_0 \tag{8}$$

so that

$$n_i = n_0 u_B \left( -\frac{2e\bar{\phi}}{M} \right)^{-1/2}. \tag{9}$$

Eqs. (6) and (9) are combined to obtain Poisson's equation

$$\frac{d^2\bar{\phi}}{dx^2} = -\frac{\xi e n_0 u_B}{\epsilon_0} \left( -\frac{2e\bar{\phi}}{M} \right)^{-1/2}. \tag{10}$$

This is the equation used in the classical Child-Langmuir theory, with the space-charge reduced by the factor $\xi$, which can be easily integrated, as many text books show (see for instance [1, 2]). The solution reads

$$\bar{\phi}(x) = \bar{V} \left( \frac{x}{s_m} \right)^{\frac{4}{3}} \tag{11}$$

$$n_i(x) = -\frac{4}{9} \frac{\epsilon_0 \bar{V}}{\xi e s_m^2} \left( \frac{x}{s_m} \right)^{-\frac{2}{3}}, \tag{12}$$

where

$$\bar{V} = -\left( \frac{9\xi e n_0 u_B}{4\epsilon_0} \right)^{2/3} \left( \frac{2e}{M} \right)^{-1/3} s_m^{4/3}, \tag{13}$$

is the time-averaged voltage on the electrode at $x = s_m$. The boundary conditions imposed in these solutions are $\bar{\phi}(x = 0) = 0$ and $\bar{E}(x = 0) = 0$, and we note that $\bar{V} < 0$ so that $n_i$ and $s_m$ are always positive. Eq. (13) reduces to the usual collisionless DC Child-Law

when $\xi = 1$, but as it can be seen, the sheath size $s_m$ will increase significantly when $\xi$ decreases, i.e. when the electrons transiently neutralize the positive space charge for part of the radiofrequency cycle.

Now consider the situation where the electrode voltage varies in time and we wish to calculate the sheath potential at some instant. Then, using our step-front electron sheath model, the sheath region is divided into a quasi-neutral region that ends at $x = s(t)$, and a positive space charge region for $x > s(t)$ where

$$\frac{dE}{dx} = \frac{\rho}{\epsilon_0} = \frac{en_i}{\epsilon_0} = -\frac{4}{9}\frac{\bar{V}}{\xi s_m^2}\left(\frac{x}{s_m}\right)^{-\frac{2}{3}}, \tag{14}$$

using Eq. (12). This equation can be integrated once to find the time and space varying electric field, using the boundary condition at $E(x = s) = 0$, yielding

$$E(x,t) = -\frac{4}{3}\frac{\bar{V}}{\xi s_m}\left[\left(\frac{x}{s_m}\right)^{\frac{1}{3}} - \left(\frac{s}{s_m}\right)^{\frac{1}{3}}\right], \tag{15}$$

in the region where $s \leq x \leq s_m$. A second integration gives the time and space varying potential in the same region as

$$\phi(x,t) = \frac{\bar{V}}{\xi}\left[\left(\frac{x}{s_m}\right)^{\frac{4}{3}} - \frac{4}{3}\left(\frac{s}{s_m}\right)^{\frac{1}{3}}\frac{x}{s_m} + \frac{1}{3}\left(\frac{s}{s_m}\right)^{\frac{4}{3}}\right], \tag{16}$$

so that the instantaneous voltage at the electrode (at $x = s_m$) is

$$V(t) = V_0\left[1 - \frac{4}{3}\left(\frac{s}{s_m}\right)^{\frac{1}{3}} + \frac{1}{3}\left(\frac{s}{s_m}\right)^{\frac{4}{3}}\right], \tag{17}$$

where we have defined the maximum voltage $V_0 = \bar{V}/\xi$, which occurs when $s = 0$. Hence we can write

$$\xi = \frac{\bar{V}}{V_0} \tag{18}$$

$$= \frac{\langle V(t)\rangle}{V_0} \tag{19}$$

$$= \left\langle 1 - \frac{4}{3}\left(\frac{s}{s_m}\right)^{\frac{1}{3}} + \frac{1}{3}\left(\frac{s}{s_m}\right)^{\frac{4}{3}}\right\rangle. \tag{20}$$

The value of $\xi$ is therefore entirely defined by the sheath motion waveform, and consequently, as we shall see in the next section, by the radiofrequency current waveform.

To relate the sheath voltage and the sheath position to the radiofrequency current, we simply note that within this model the current passing through the sheath is entirely displacement at the electrode, so that

$$J(t) = \epsilon_0 \left. \frac{\partial E}{\partial t} \right|_{x=s_m} \tag{21}$$

$$= -\frac{4}{3} \frac{\epsilon_0 V_0}{s_m} \frac{d}{dt} \left[ 1 - \left( \frac{s}{s_m} \right)^{\frac{1}{3}} \right]. \tag{22}$$

There is a physical constraint that $J = 0$ when $s = 0$ and $s = s_m$. We choose the convention that $s(t = 0) = 0$. The current waveform must be chosen to be consistent with this convention, but this imposes no physically significant restrictions. Hence, the sheath position is defined solely by the radiofrequency current waveform $J(t)$,

$$\frac{s}{s_m} = \left[ \frac{3}{4} \frac{s_m}{\epsilon_0 V_0} \int_0^t J(t) dt \right]^3. \tag{23}$$

Since $s/s_m$ has a maximum value of unity, we must satisfy

$$\max \left( \frac{3}{4} \frac{s_m}{\epsilon_0 V_0} \int_0^t J(t) dt \right) = 1. \tag{24}$$

This equation defines the current-voltage characteristic of the collisionless sheath and is particularly useful for the widely-used circuit model descriptions of capacitive discharges.

## B. Collisional sheaths

### 1. *The fields*

If we now consider an intermediate pressure regime in which the sheath is collisional, the ion motion becomes limited by collisions and the ion fluid velocity in the sheath becomes a function of the local time-averaged electric field [1, 2],

$$u_i = \frac{2e\lambda_i}{\pi M |u_i|} \bar{E} \tag{25}$$

where $\lambda_i$ is the ion-neutral mean free path. Using ion flux conservation in the sheath, we obtain the ion density in the sheath as a function of the electric field,

$$n_i = \frac{n_0 u_B}{(2e\lambda_i \bar{E}/(\pi M))^{1/2}}. \tag{26}$$

6

Gauss's law,

$$\frac{d\bar{E}}{dx} = \frac{e\xi n_i}{\epsilon_0} = \frac{e\xi n_0 u_B}{\epsilon_0 (2e\lambda_i \bar{E}/(\pi M))^{1/2}}, \tag{27}$$

is integrated to obtain the time-averaged electric field in the sheath,

$$\bar{E}(x) = \left[\frac{3e\xi n_0 u_B}{2\epsilon_0 (2e\lambda_i/(\pi M))^{1/2}}\right]^{2/3} x^{2/3}, \tag{28}$$

where we have used $\bar{E}(0) = 0$ (the electric field at the plasma-sheath interface) as a boundary condition. A second integration gives the time-averaged potential in the sheath

$$\bar{\phi}(x) = -\frac{3}{5}\left[\frac{3e\xi n_0 u_B}{2\epsilon_0 (2e\lambda_i/(\pi M))^{1/2}}\right]^{2/3} x^{5/3}, \tag{29}$$

where we have again chosen $\bar{\phi}(0) = 0$. We can now rewrite this expression in the following way,

$$\bar{\phi}(x) = \bar{V}\left(\frac{x}{s_m}\right)^{5/3}, \tag{30}$$

with

$$\bar{V} = -\frac{3}{5}\left[\frac{3e\xi n_0 u_B}{2\epsilon_0 (2e\lambda_i/(\pi M))^{1/2}}\right]^{2/3} s_m^{5/3}. \tag{31}$$

This is the collisional radiofrequency Child-Law. Combining Eqs (26), (28) and (31) we obtain the ion density in the sheath,

$$n_i(x) = -\frac{10}{9}\frac{\epsilon_0 \bar{V}}{\xi e s_m^2}\left(\frac{x}{s_m}\right)^{-\frac{1}{3}}. \tag{32}$$

Following the same procedure as in the collisionless sheath case we obtain the time-varying fields in the sheath, starting from Gauss's law,

$$\frac{dE}{dx} = \frac{\rho}{\epsilon_0} = \frac{en_i}{\epsilon_0} = -\frac{10}{9}\frac{\bar{V}}{\xi s_m^2}\left(\frac{x}{s_m}\right)^{-\frac{1}{3}}, \tag{33}$$

such that using $E(x = s) = 0$ we have

$$E(x,t) = -\frac{15}{9}\frac{\bar{V}}{\xi s_m}\left[\left(\frac{x}{s_m}\right)^{\frac{2}{3}} - \left(\frac{s}{s_m}\right)^{\frac{2}{3}}\right], \tag{34}$$

and

$$\phi(x,t) = \frac{\bar{V}}{\xi}\left[\left(\frac{x}{s_m}\right)^{\frac{5}{3}} - \frac{5}{3}\left(\frac{s}{s_m}\right)^{\frac{2}{3}}\frac{x}{s_m} + \frac{2}{3}\left(\frac{s}{s_m}\right)^{\frac{5}{3}}\right]. \tag{35}$$

The instantaneous voltage at the electrode becomes

$$V(t) = V_0\left[1 - \frac{5}{3}\left(\frac{s}{s_m}\right)^{\frac{2}{3}} + \frac{2}{3}\left(\frac{s}{s_m}\right)^{\frac{5}{3}}\right], \tag{36}$$

and consequently

$$\xi = \frac{\bar{V}}{V_0} = \left\langle 1 - \frac{5}{3}\left(\frac{s}{s_m}\right)^{\frac{2}{3}} + \frac{2}{3}\left(\frac{s}{s_m}\right)^{\frac{5}{3}}\right\rangle. \tag{37}$$

*2. Current-voltage characteristic of the sheath*

The current passing through the sheath is now

$$J(t) = \epsilon_0 \left. \frac{\partial E}{\partial t} \right|_{x=s_m} \tag{38}$$

$$= -\frac{15}{9} \frac{\epsilon_0 V_0}{s_m} \frac{d}{dt} \left[ 1 - \left( \frac{s}{s_m} \right)^{\frac{2}{3}} \right], \tag{39}$$

such that if $s(t=0) = 0$ we obtain

$$\frac{s}{s_m} = \left[ \frac{9}{15} \frac{s_m}{\epsilon_0 V_0} \int_0^t J(t) dt \right]^{3/2}. \tag{40}$$

and the following condition must be satisfied:

$$\max \left( \frac{9}{15} \frac{s_m}{\epsilon_0 V_0} \int_0^t J(t) dt \right) = 1. \tag{41}$$

This equation defines the current-voltage characteristic of the collisional sheath.

## III.   RESULTS FOR A SHEATH DRIVEN BY A PULSED CURRENT WAVE-FORM

The above expressions are completely general (within our fundamental approximation) and therefore independent of the radiofrequency current waveform used. In reference [13], single-frequency and dual-frequency sinusoidal waveforms were analysed in the collisionless case and compared to Particle-In-Cell (PIC) simulations, showing excellent agreement. A pulsed-current waveform was also proposed as an example. In this paper we treat this latter case for both collisionless and collisional sheaths, with a discharge driven by a current density of the form

$$J(t) = J_0 \left( \frac{t}{t_w} \right) \exp \left( \frac{1}{2} - \frac{1}{2} \frac{t^2}{t_w^2} \right), \tag{42}$$

where the function has positive and negative extrema of $\pm J_0$, separated in time by an interval $2t_w$. We assume that this pulse is repeated at intervals $t_p$, supposed large enough that there is no appreciable interaction between successive pulses ($t_p \gg t_w$). This type of waveform has been recently proposed for self-bias generation and control on electrodes of equal areas [11]. As we shall see, the voltage waveform is close to a Gaussian peak in this case, such that the sheath voltage is small during most of the radiofrequency cycle and $\xi$ is expected

8

to be small when $t_p \gg t_w$. To solve the model, we start by evaluating the integral of the radiofrequency current,

$$\int_0^t J(t)dt = J_0 t_w \exp\left(\frac{1}{2}\right)\left[1 - \exp\left(-\frac{1}{2}\frac{t^2}{t_w^2}\right)\right] \tag{43}$$

$$\max\left(\int_0^t J(t)dt\right) = J_0 t_w \exp\left(\frac{1}{2}\right) \tag{44}$$

such that for the collisionless sheath case, using Eqs (23) and (24), we immediately obtain the sheath position waveform and the current-voltage characteristic,

$$\frac{s(t)}{s_m} = \left[1 - \exp\left(-\frac{1}{2}\frac{t^2}{t_w^2}\right)\right]^3 \tag{45}$$

$$1 = \frac{3}{4}\frac{s_m J_0 t_w \exp\left(\frac{1}{2}\right)}{\epsilon_0 V_0} \tag{46}$$

The value of $\xi$ is then easily obtained,

$$\xi = \left\langle 1 - \frac{4}{3}\left(\frac{s}{s_m}\right)^{\frac{1}{3}} + \frac{1}{3}\left(\frac{s}{s_m}\right)^{\frac{4}{3}} \right\rangle \tag{47}$$

$$\approx \frac{1}{2t_p}\int_{-\infty}^{\infty}\left\{1 - \frac{4}{3}\left[1 - \exp\left(-\frac{1}{2}\frac{t^2}{t_w^2}\right)\right] + \frac{1}{3}\left[1 - \exp\left(-\frac{1}{2}\frac{t^2}{t_w^2}\right)\right]^4\right\}dt \tag{48}$$

$$= \frac{t_w}{t_p}\sqrt{\pi}\left(1 - \frac{2}{9}\sqrt{6} + \frac{1}{12}\sqrt{2}\right) \tag{49}$$

where we have used the fact that $t_p \gg t_w$ so that the integration can be performed from $-\infty$ to $\infty$. A similar analysis can be done for the collisional sheath, with the following results

$$\frac{s(t)}{s_m} = \left[1 - \exp\left(-\frac{1}{2}\frac{t^2}{t_w^2}\right)\right]^{3/2} \tag{50}$$

$$1 = \frac{9}{5}\frac{s_m J_0 t_w \exp\left(\frac{1}{2}\right)}{\epsilon_0 V_0} \tag{51}$$

$$\xi \approx \frac{1}{2t_p}\int_{-\infty}^{\infty}\left\{1 - \frac{5}{3}\left[1 - \exp\left(-\frac{1}{2}\frac{t^2}{t_w^2}\right)\right] + \frac{2}{3}\left[1 - \exp\left(-\frac{1}{2}\frac{t^2}{t_w^2}\right)\right]^{5/2}\right\}dt \tag{52}$$

Figure 2 shows the evolution of the parameter $\xi$ as a function of $t_p/t_w$. The solid line is given by Eq. (49) for collisionless sheaths, while the points are numerical integrations of Eq. (52) for collisional sheaths, which could not be integrated analytically. Consistent with the voltage waveforms in figure 3, $\xi$ is almost independent of the model used. When $t_p/t_w$ increases, the voltage pulse gets shorter and as a consequence the portion of the time where the electrons fill the sheath gets larger. The time-averaged electron space charge therefore becomes comparable to the time-independent ion space charge and consequently $\xi$ goes to

zero, leading to a very large maximum sheath thickness for a given time-averaged voltage (according to Eqs. (13) and/or (31)).

The time-dependent results of the collisionless and collisional sheath models are compared in figure 3. The sheath position as a function of the normalized time is shown in the top figure while the voltage waveform is shown in the bottom figure. Significant differences are seen in the sheath position evolution, but these differences are greatly smoothed out in the voltage waveforms. Actually the voltage waveforms are reasonably close to a Gaussian pulse, shown in red in the figure. A Gaussian voltage pulse would be obtained for a truly capacitive sheath (a sheath modelled by a linear capacitor), for which the current pulse is proportional to the time derivative of the voltage pulse. The departure from the Gaussian accounts for the non-linear response of the moving sheath.

Although the voltage waveform seems mostly independent of the model used (collisional or collisionless), the maximum sheath thickness for a given time-averaged voltage is a function of the model used, and will significantly vary with collisionality. This is illustrated in figure 4 where the maximum sheath size, $s_m$, is plotted as a function of the ion-neutral mean free path $\lambda_i$. This figure has been obtained for argon ions with $n_0 = 10^{16}$ m$^{-3}$, $T_e = 3$ V, $\xi = 0.5$, and $\overline{V} = 100$ V. The solid line is from the collisional theory, Eq. (31), and the dashed-line is the constant value of the collisionless theory, Eq. (13). The collisional theory must be used for short mean free path, but as it can be seen, the two curves intersect at $\lambda_i = 0.0006$, which may be seen as the limit where the collisional sheath theory starts to fail. Alternatively, one may consider that the collisional theory should be used when $\lambda_i < s_m$; this occurs for $\lambda_i = 0.0027$ in the example of figure 4 (the gray area indicates the region where $\lambda_i > s_m$).

## IV. CONCLUSION

In this paper, we have rehearsed the sheath model presented previously in reference [13] and extended it to the case of collisional sheaths in the intermediate pressure regime. The model relies on a simplifying assumption and is easily solved for any radiofrequency waveform, in the limit where the ions only respond to time-averaged fields. To illustrate the practical use of this model, we chose a pulsed-current waveform of interest for modern experiments. In this case, we have found a significant difference in the time-resolved sheath position between collisional and collisionless sheath. This difference is not as pronounced in

the voltage waveform. However, the maximum sheath thickness for a given time-averaged voltage depends on the sheath collisionality, as seen in Eq. (31).

# REFERENCES

[1] M. A. Lieberman and A. J. Lichtenberg, *Principles of Plasma Discharges and Materials Processing*, 2nd ed. (Wiley-Interscience, 2005).

[2] P. Chabert and N. Braithwaite, *Physics of Radio-Frequency Plasmas* (Cambridge University Press, 2011).

[3] P. Chabert, J. A. Monreal, J. Bredin, L. Popelier, and A. Aanesland, Phys. Plasmas **19**, 073512 (2012).

[4] V. S. von der Gathen, L. Schaper, N. Knake, S. Reuter, K. Niemi, T. Gans, and J. Winter, Journal of Physics D: Applied Physics **41**, 194004 (2008).

[5] J. Waskoenig, K. Niemi, N. Knake, L. M. Graham, S. Reuter, V. S. von der Gathen, and T. Gans, Plasma Sources Sci. Technol. **19**, 045018 (2010).

[6] C. Lazzaroni, P. Chabert, M. A. Lieberman, A. J. Lichtenberg, and A. Leblanc, Plasma Sources Sci. Technol. **21**, 035013 (2012).

[7] V. Godyak, *Soviet Radiofrequency Discharge Research*, edited by V. Delphic Associates, Fall Church (Delphic Associates, Fall Church, VA, 1986).

[8] M. A. Lieberman, IEEE Trans. Plasma Sci. **16**, 638 (1988).

[9] J. Robiche, P. C. Boyle, M. M. Turner, and A. R. Ellingboe, J. Phys. D: Appl. Phys. **36**, 1810 (2003).

[10] B. G. Heil, U. Czarnetzki, R. Brinkmann, and T.Mussenbrock, J. Phys. D: Appl. Phys. **41**, 165202 (2008).

[11] T. Lafleur, Plasma Sources Science and Technology **25**, 013001 (2016).

[12] U. Czarnetzki, Phys. Rev. E **88**, 063101 (2013).

[13] M. M. Turner and P. Chabert, Applied Physics Letters **104**, 164102 (2014).

[14] T. Lafleur, P. Chabert, M. M. Turner, and J. P. Booth, Plasma Sources Science and Technology **22**, 065013 (2013).
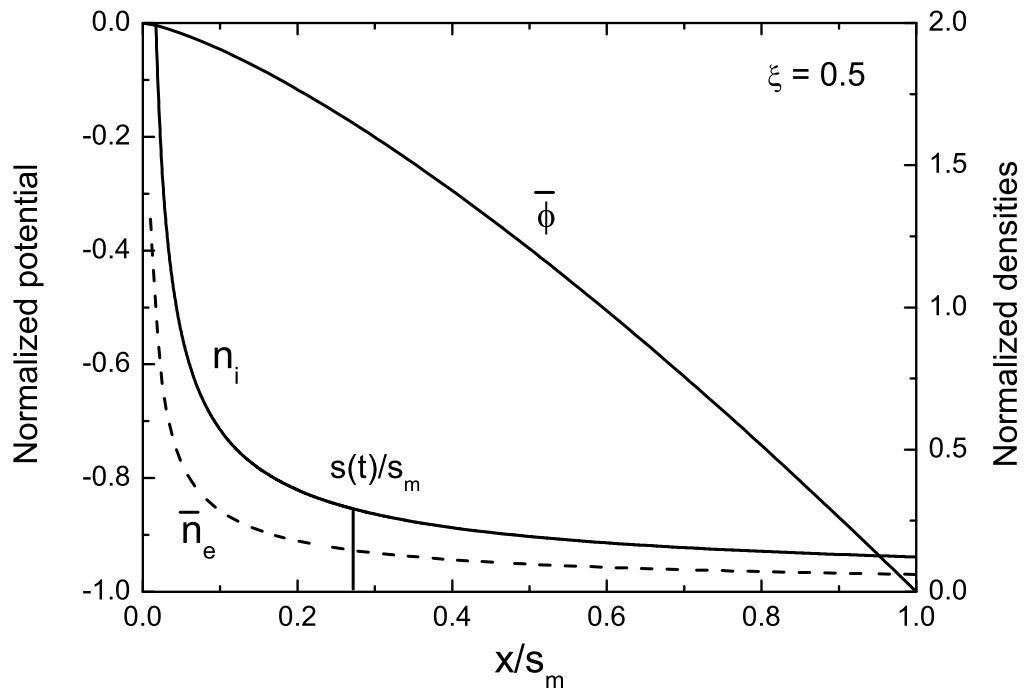
FIG. 1. Time-averaged densities and potential in the sheaths for $\xi = 0.5$ in the collisionless case, after Eqs. (11) and (12). The vertical line at $s(t)/s_m$ represents the instantaneous sheath position.
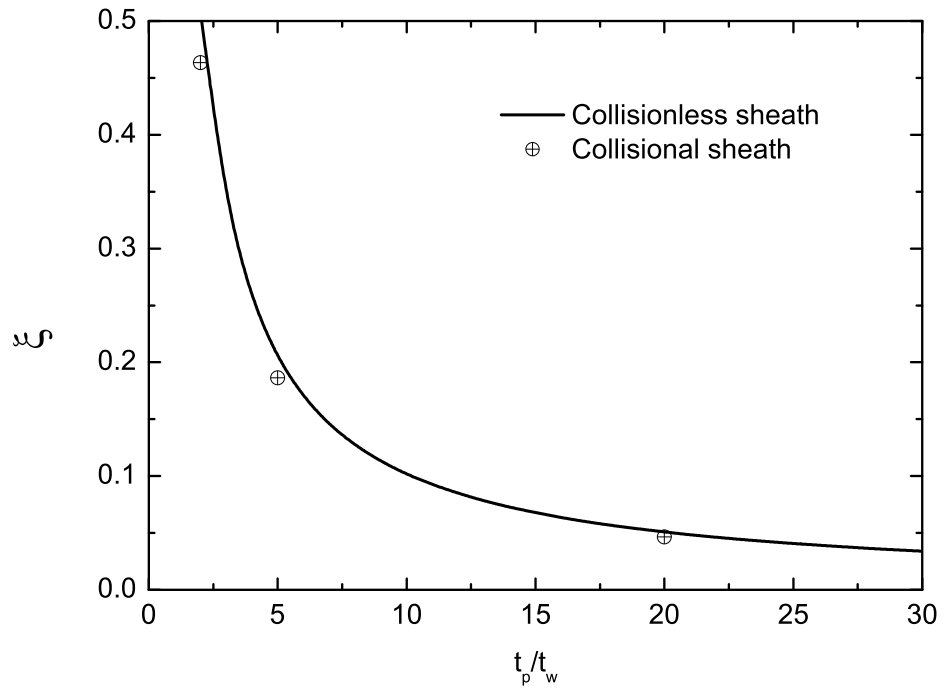
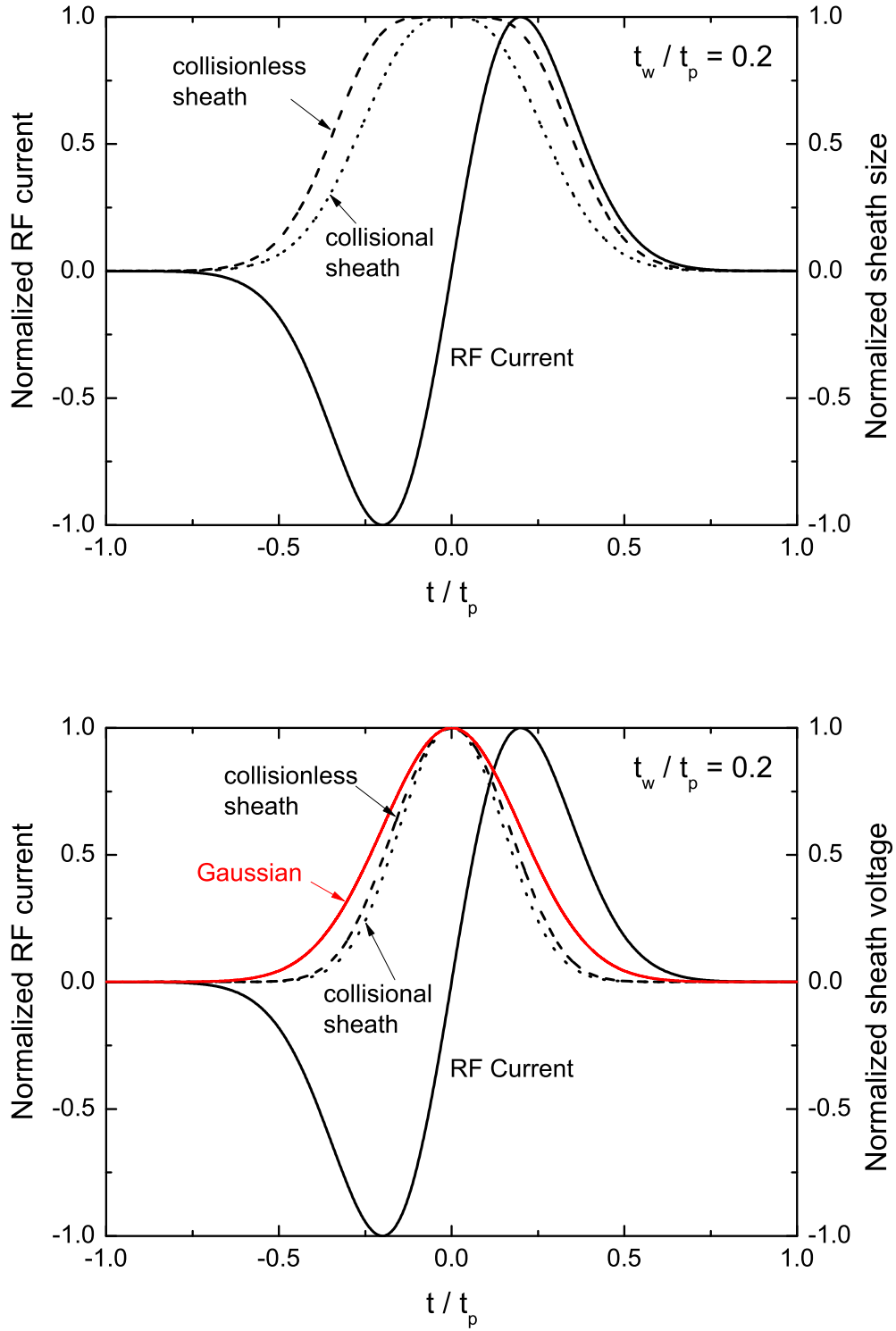FIG. 2. Evolution of the parameter $\xi$ as a function of $t_p/t_w$.

FIG. 3. Time variation of the sheath sizes (top) and the voltages (bottom) for a pulsed-current from Eq. (42). The dashed lines are for collisionless sheaths while the dotted lines are for collisional sheaths. The read line in the bottom figure is the voltage profile expected for a linear capacitor.
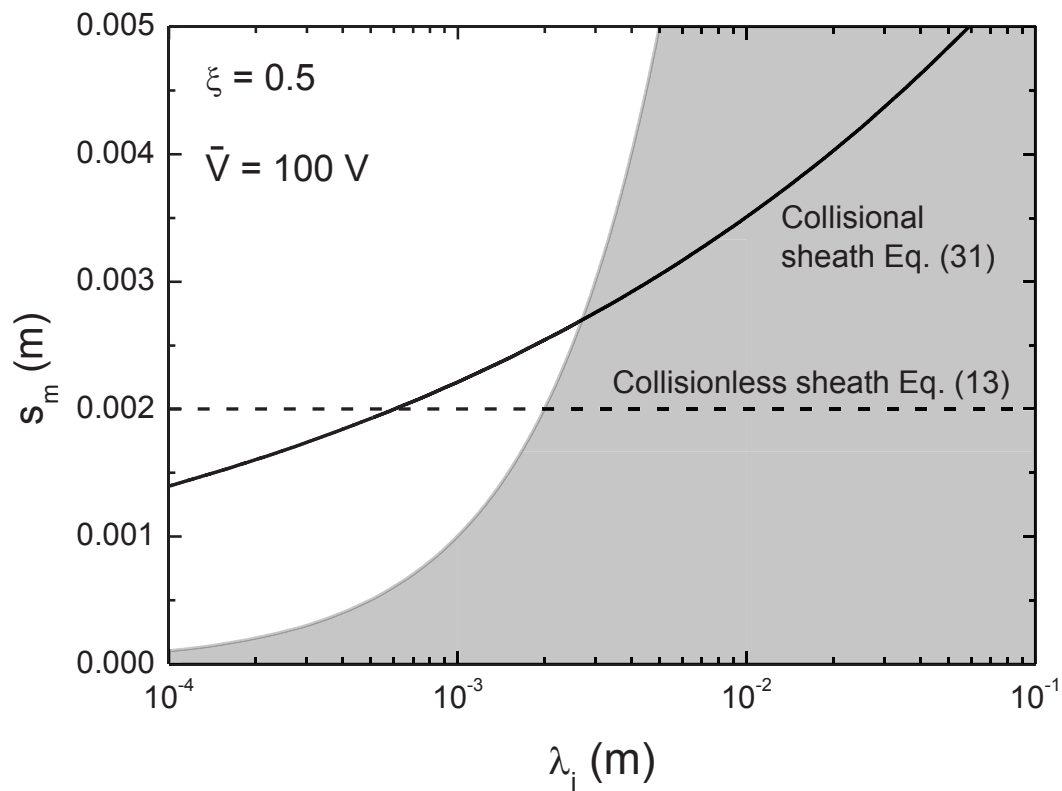
15

FIG. 4. Maximum sheath size as a function of the ion-neutral mean free path. The solid line is from the collisional theory, Eq. (31), and the dashed-line is the constant value of the collisionless theory, Eq. (13). The gray area is the region where $\lambda_i > s_m$. This figure has been obtained for argon ions with $n_0 = 10^{16}$ m$^{-3}$, $T_e = 3$ V, $\xi = 0.5$, and $\overline{V} = 100$ V.